# Optical analogue of black and white gravitational holes

Eric Plum<sup>1,a)</sup>, Anton N. Vetlugin<sup>2</sup>, Baurzhan Salimzhanov<sup>1</sup>, Nikolay I. Zheludev<sup>1,2</sup> and Nina Vaidya<sup>3,a)</sup>

In general relativity, a gravitational "white hole" is a hypothetical region of space that cannot be entered from outside. It is the reverse of a "black hole", from which light and information cannot escape. We report an optical device exhibiting intriguing similarities. It will either totally absorb (optical black hole) or totally reject (optical white hole) light of any wavelength, depending on its polarization. The device's functionality is based on the formation of a standing wave from the wavefront of spatially coherent incident radiation. Interaction of the standing wave with a thin absorber enables coherent perfect absorption and transmission, while polarization sensitivity is derived from the geometrical phase of the interfering beams. We provide experimental proof-of-principle demonstrations and show that the device operates as a black and white hole for orthogonal polarizations of the incident light. From a remote point, it will look like a gravitational black or white hole depending on the polarization of light. In principle, the optical black and white hole device can operate as a deterministic absorber or rejector throughout the entire electromagnetic spectrum irrespective to the light intensity. Broadband absorbers and rejectors can be useful for energy harvesting, detection, stealth technologies, and redistribution of light.

**Keywords:** Coherent perfect absorption, temporal and spatial coherence, interference, absorption, reflection, geometric phase

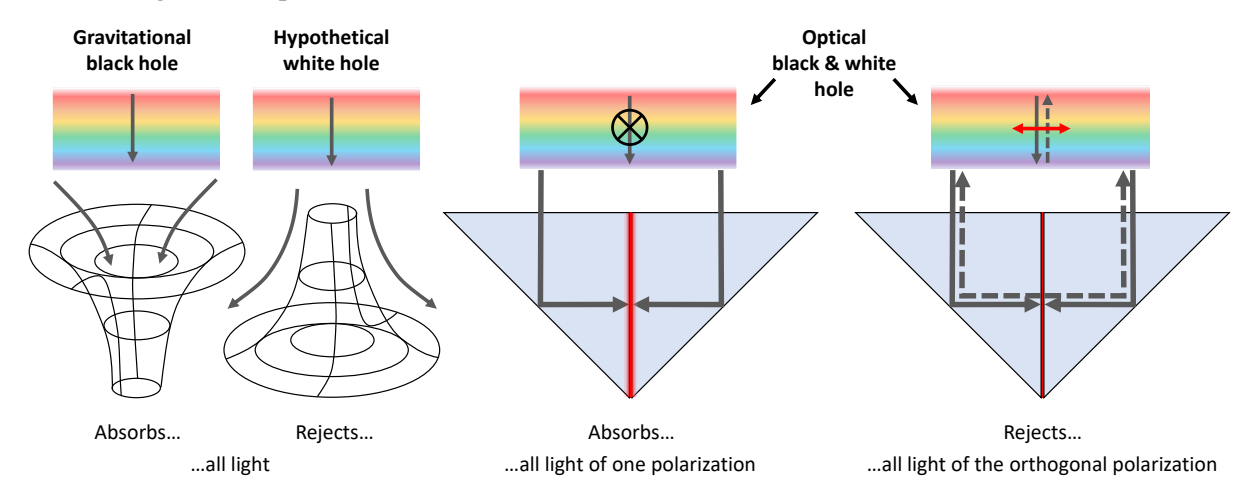


Figure 1. Astronomical gravitational black holes swallow everything that crosses their event horizon. Their counterpart, the white hole, rejects everything and it is hypothesized that its event horizon cannot be crossed from outside. The "optical black and white holes" absorb and reject all light depending on its polarization.

<sup>&</sup>lt;sup>1</sup> Optoelectronics Research Centre and Centre for Photonic Metamaterials, University of Southampton, Highfield, Southampton SO17 1BJ, United Kingdom

<sup>&</sup>lt;sup>2</sup> Centre for Disruptive Photonic Technologies, SPMS, TPI, Nanyang Technological University, Singapore 637371, Singapore

<sup>&</sup>lt;sup>3</sup> Faculty of Engineering and Physical Sciences, Boldrewood Innovation Campus, University of Southampton, Southampton SO16 7QF, United Kingdom

a) Authors to whom correspondence should be addressed: <a href="mailto:erp@orc.soton.ac.uk">erp@orc.soton.ac.uk</a> and <a href="mailto:n.vaidya@soton.ac.uk">n.vaidya@soton.ac.uk</a>

#### Introduction

All light that enters a gravitational singularity known as a black hole is absorbed. Similarly, all light that tries to enter a white hole is rejected (Fig. 1). The electromagnetic inaccessibility of these objects has motivated the study of analogue systems exhibiting similar characteristics from fluid dynamics<sup>1</sup>, acoustics<sup>2</sup>, and Bose-Einstein condensates<sup>3</sup> to linear<sup>4,5</sup> and nonlinear<sup>6-9</sup> optics. In particular, the previously proposed linear optical black holes have relied on metamaterials to imitate curved spacetime with a complex refractive index profile, making their implementation challenging.<sup>4,5</sup>

Here we introduce the concept and provide a proof-of-principle demonstration of an "optical black and white hole" that deterministically absorbs all light of one linear polarization while rejecting all light of the orthogonal polarization. In contrast to the prior linear optical photonic black holes, it relies on coherent perfect absorption<sup>10</sup> enabled by spatial coherence and interference and has a simple geometry that can be implemented using available materials.

## Perfect absorption and rejection through interference

While absorbers for a single beam of light have been studied for a long time, <sup>11-15</sup> since 2012 it become well-known that interference of two coherent light beams on a thin absorber can eliminate the Joule losses of optical energy or, in contrast, can lead to total, deterministic absorption of light. <sup>16-18</sup>

Consider a thin light-absorbing film of sub-wavelength thickness. The result of interference of two temporally coherent counter-propagating incident beams of the same intensity on such a film is illustrated by two opposite cases. In the first, a standing wave is formed with zero electric field, a node arising from destructive interference, at the position of the absorbing film. As the film is much thinner than the optical wavelength, its electric-dipole interaction with the electromagnetic field is negligible and the absorber will appear to be transparent for both incident waves. (The amplitude of the magnetic field is at a maximum here, but magnetic dipole transitions are typically much less efficient than electric dipole transitions, so may be neglected in this simplified picture.) In the second case, the film is at a position of constructive interference, an electric field maximum (anti-node), where the electric-dipole interaction is strong and the associated absorption becomes very efficient.

Irrespective of the mechanism of absorption, an analysis of such interference <sup>17</sup> shows that perfect deterministic transmission and absorption of light can be achieved in a thin (relative to the wavelength) absorber if, for traveling wave illumination, its reflectivity from either side is ½, and ½ of optical power is absorbed in the film. For fundamental reasons, an infinitesimally thin film cannot absorb more than half of the energy from a traveling wave, <sup>19,20</sup> and a very close approximation of this limit is possible with natural materials (e.g., multilayered graphene<sup>21</sup> or thin metal layers <sup>22-24</sup>) or/and metamaterial structuring of films of nanoscale thicknesses <sup>16,25</sup>. If waves incident on both sides of such an absorber interfere constructively (destructively) at the absorber, as described in the previous paragraph, then reflected and transmitted waves on either side of the absorber will have equal amplitude and a  $\pi$  (0) phase difference, resulting in complete cancellation (constructive interference) of all outgoing fields and thus complete absorption (transmission) of all incident light. In a bigger picture that includes the thermal radiation of the film, the absorbed energy that may be retained and utilized from the absorber depends on the temperatures of the absorber and the source of light; the Landsberg thermodynamic limit <sup>26</sup> caps the efficiency of radiative energy utilization at a value slightly lower than 100%.

The regime of nearly perfect absorption in a standing wave has been experimentally demonstrated with classical light, <sup>16</sup> single<sup>27</sup> and entangled photons<sup>28</sup> and has been used in applications such as all-optical light modulation including ultrafast optical pulses, <sup>29</sup> single photon optical switching<sup>30</sup>, data processing in classical<sup>31</sup> and quantum<sup>32</sup> networks, and image recognition.<sup>33</sup>

So far, we discussed perfect absorptivity and transmissivity arrangements involving two coherent counter-propagating beams. The interference required for perfect broadband absorption and transmission can be constructed by splitting an incident beam of light into two coherent beams using a

beam splitter and directing these two beams to opposite sides of the absorber. However, this is not possible without a complex and bulky arrangement of multiple mirrors making such absorbers impractical.

The main purpose of the present work is to demonstrate that interference on a thin absorber can lead to nearly perfect absorption of thermal or laser light from a broadband source exploiting its spatial coherence, i.e., uniformity of the phase of the wavefront. Spatial coherence is a characteristic feature of single-mode laser light but is also a feature of remote sources. Indeed, all waves are spatially coherent on sufficiently small length scales. For instance, light with wavelength  $\lambda = 500$  nm that comes from the closest star outside the solar system, Proxima Centauri (star diameter  $\delta = 214550$  km), located at a distance D=4.25 light-years from Earth is spatially coherent across a wavefront diameter of d =  $0.16\lambda D/\delta = 15$  m. Light from a similar star located within the Andromeda Galaxy, the closest major galaxy at a distance of 2.54 million light-years, is spatially coherent across a wavefront diameter of 9000 km (e.g., from the UK to Japan).

For the conceptual design that we propose in this work, consider two mirrors set at a right angle to each other and a thin absorber placed along the bisector plane separating them (Fig. 2). If the arrangement is narrower than the spatial coherence area of the incident radiation, light rays directed by the mirrors onto opposite sides of the same absorber area from non-overlapping parts of the incident beam will be coherent and therefore interfere.

The type of interference is determined by the polarization of light. In the case of light that is linearly polarized in the plane of the absorber (perpendicular to the plane of incidence, i.e., s-polarization), the polarization state and relative phase of the waves propagating towards either side of the absorber do not change upon reflection: beams arriving on the opposite sides of the absorber are in phase and they interfere constructively (Fig. 2a). Hence, this arrangement enables total absorption of any spectral component of the incident light: perfect broadband absorption.

However, if the incident light is polarized perpendicular to the plane of the absorber (parallel to the plane of incidence, i.e., p-polarization), upon reflection the electric field vector rotates  $+90^{\circ}$  on one of the mirrors and  $-90^{\circ}$  on the other (Fig. 2b). These polarization changes may be represented as trajectories between antipodal points on the Poincaré sphere, in opposite directions along its equator. As a trajectory around the whole equator is associated with a Pancharatnam–Berry phase  $^{35}$  of  $\pi$ , opposite trajectories along half of the equator are associated with phases of  $\pm \pi/2$ . Accordingly, the beams accrue a geometric phase difference of  $\pi$  upon reflection and interfere destructively on the absorber, resulting in electric field cancellation and thus negligible absorption: a perfect arrangement for total transmission. Due to the geometric nature of the phase difference, the effect does not depend on the wavelength. Therefore, an incident light beam polarized perpendicular to the plane of the absorber will suffer no absorption for any spectral component, resulting in the reflection of all light by the device.

The geometric phase difference may also be understood from symmetry considerations. It arises from the redirection of incident light from co-propagating to counter-propagating. In the case of spolarization, the device geometry including *electric* fields is entirely symmetric with respect to the plane of the absorber (Fig. 2a), resulting in constructive interference of the electric fields. In contrast, for polarization the device geometry including *magnetic* fields is entirely symmetric with respect to the absorber (i.e., the magnetic fields in Fig. 2b behave like the electric fields in Fig. 2a), resulting in constructive interference of the magnetic fields. Due to the right-handed arrangement of the wave vector, electric field, and magnetic field of a traveling electromagnetic wave, counterpropagation implies that constructive interference of one field is accompanied by destructive interference of the other.

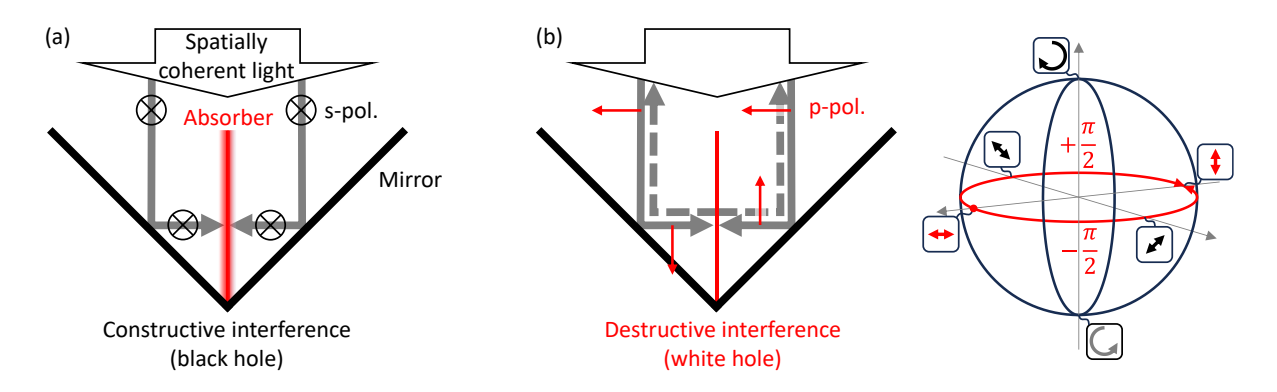


Figure 2. Mechanism of complete absorption and complete rejection of light. Spatially coherent and normally incident (a) spolarized light interferes constructively on a thin film absorber placed at the bisector plane separating two mirrors set at a right angle to each other, resulting in coherent absorption, while (b) p-polarized light interferes destructively, resulting in coherent transmission, in principle with unlimited bandwidth. Destructive interference of incident p-polarized light occurs due to a geometric phase difference of  $\pi$  that arises from the rotation of the polarization state upon reflection as illustrated on the Poincaré sphere. Constructive interference of incident s-polarized light is due to the absence of any polarization change and associated geometric phase.

## **Experiment**

The optical black and white hole device studied here consists of two identical 90° prisms manufactured from BK7 glass (Precision Optical Inc.) and polished to 80 nm surface flatness. The height of the prisms is 15 mm while their legs are 21.3 mm wide. A 20 nm layer of chromium was deposited on a leg of one prism by thermal evaporation before the device was assembled by placing the chromium-coated prism face in contact with the uncoated prism, as shown in Fig. 1, with glass index matching liquid covering the contact area to avoid any air gap, i.e., to ensure that the refractive index is the same on either side of the chromium film. For this proof-of-principle demonstration, the mirror reflections within the device occur by total internal reflection at the glass-air interfaces of the prism hypotenuses and we chose chromium as the absorber material as it provides close to the desired absorption and reflection characteristics in a film of deeply subwavelength thickness in the near-infrared part of the spectrum where the proof-of-principle demonstration is performed (Supplementary Sections S1.1, S1.2 and Figure S6).

As illustrated by Supplementary Figure S7, the experiments were performed with the output of a continuous wave C+L band tunable laser (HP 8168F) with a spectral width of 100 kHz, which was collimated by a fiber collimator, and directed towards the device such that the incident laser beam was centered on the boundary between the prisms. Reflected light then passed through an analyzer that selected one of the eigenpolarizations (s or p-polarization with electric field parallel or perpendicular to the absorbing film) before being detected by an optical power meter. We measured the power r of the reflected light as a fraction of the incident optical power  $r_0$  to determine the reflectivity of the device,  $R_{\rm M} = r/r_0$ .

A small, fixed angle of incidence of  $\beta \approx 2^\circ$  within the plane of the chromium film and a ~1 mm slit were used to separate incident and reflected light, which had a Gaussian distribution with  $1/e^2$  diameter of ~7 mm in the plane perpendicular to the chromium film (Supplementary Figure S7). This spaces multiple reflections by more than the slit width, avoiding any additional interference or Fabry-Pérotcavity effects, allowing us to remove reflections from the glass air interface analytically. To show the performance of anti-reflection coated prisms, the 4% reflectivity of the glass air interface has been removed from the measured reflectivity  $R_{\rm M}$ , by calculating the reflectivity with an anti-reflection

coating on the input face as  $R = 1/(\frac{0.962}{R_{\rm M}-0.04} + 0.04)$ . The absorptivity A is given by A = 1 - R. The optical paths were matched by translating one prism relative to the other using a piezo stage and optimizing the bandwidth of absorption for s-polarization, which also compensates for any slight size differences between the prisms of nominally identical size.

We investigated the dependence of reflectivity and absorptivity as functions of  $\alpha$  (Fig. 3) – the beam incident angle on the device – and laser wavelength  $\lambda$  (Fig. 4).

Fig. 3 shows the measured reflectivity and absorptivity at a wavelength of 1570 nm as a function of the angle of incidence for two incident polarizations (s and p), parallel and perpendicular to the plane of the absorbing film. At oblique incidence, a similar absorptivity of around 60% (~40% reflectivity) of the incident power is observed for both polarizations. However, as the angle of incidence approaches 0°, the absorptivity changes dramatically, approaching complete absorption (negligible rejection) for spolarization and decreasing towards minimal absorption (increasing towards complete rejection) for polarization. Arguably, the rapid angular transition to black-hole-like absorption of s-polarized light and white-hole-like rejection of p-polarized light at normal incidence may be thought of as an event horizon.

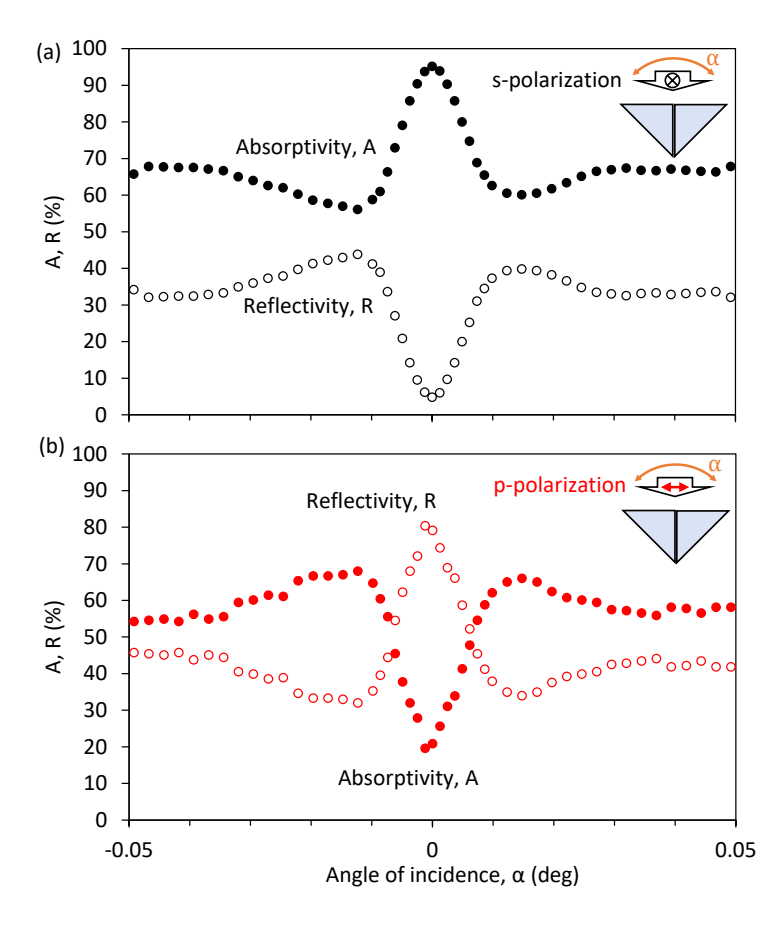


Figure 3. Observation of the optical black and white hole analogues. Measured reflectivity and absorptivity of a chromium thin film on the interface between two identical glass prisms for (a) s- and (b) p-polarized light as a function of the angle of incidence. Absorption of s-polarized light (black hole) and rejection of p-polarized light (white hole) occurs around normal incidence.

Fig. 4 shows the spectral dependence of the optical black and white hole responses. The observed reflectivity and absorptivity are spectrally flat across the tuning range of the laser, indicating that it is broadband. For the optical black hole case, we observe 91% absorption, while 85% reflectivity is

observed for the optical white hole case. Simulations illustrate traveling wave propagation towards the device for the black hole case (Fig. 4a), where negligible interference above the prisms indicates the near-complete absence of reflected light. In contrast, for the white hole case (Fig. 4b), almost all light is rejected by the device, resulting in almost equal amplitudes of light propagating towards and away from the prisms and thus the formation of a standing wave. The simulations in Fig. 4a and Fig 4b were carried out in Comsol Multiphysics for s- and p-polarized coherent plane wave illumination (λ=1570 nm, from the upper boundary) of aligned prisms with a leg length L=14 μm and refractive index 1.5, with a 320 nm thick anti-reflecting coating having refractive index 1.225 on the input face and with a 20 nm thick absorber with refractive index 4.6+4.4i. Lateral outer boundaries above the prisms are periodic and a scattering condition was used for all other outer boundaries. (Light scattering from the prism tip becomes insignificant at macroscopic prism sizes and can also be avoided by adding a reflective coating, Supplementary Section S1.4 and Supplementary Figure S5.)

We note that the ultimately broadband optical black hole and white hole responses for s- and p-polarizations that occur for perfectly aligned identical prisms, can be reversed (over a large but finite bandwidth) by introducing a relative displacement  $\Delta z = \lambda_0/2$  between the prisms, where  $\lambda_0$  is the free-space wavelength and z is the direction of normal incidence (Supplementary Section S1.3). The measurements in Fig. 4 illustrate this, they show s-polarization with  $\Delta z \approx 0$  (black hole case) and  $\Delta z \approx 800$  nm (white hole case). The tuning range of our laser is not large enough to distinguish between these ideal and approximate white/black hole configurations.

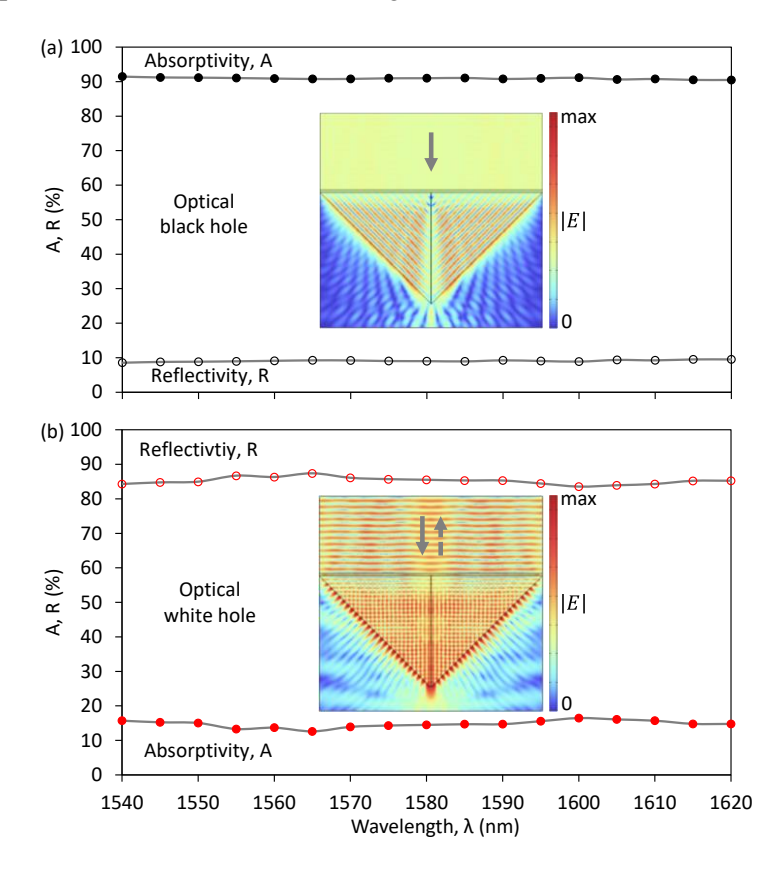


Figure 4. Broadband absorption and rejection of light by optical (a) black and (b) white holes. Measured reflectivity and absorption as a function of wavelength at normal incidence. Inset simulations illustrate the absence of reflection from the device for the black hole case (a) and the formation of a standing wave due to interference of incident and reflected light for the white hole case (b).

#### **Discussion**

While an ideal optical black and white hole is expected to deliver deterministic absorption and rejection of light, less than 100% absorptivity and reflectivity were observed in our proof-of-principle experiments. Causes of the finite absorptivity and reflectivity include diffraction at edges and flatness of faces of the prisms, as well as wavefront distortions arising from imperfect illumination optics. Calculations show that various real absorber materials can deliver very close to deterministic absorption and deterministic rejection of light over multiple octaves of the electromagnetic spectrum (Supplementary Section S1.2).

The acceptance angle within which near-complete absorption or rejection of light occurs as well as angular alignment tolerances are controlled by the size of the prisms and become large as the prism size L approaches the wavelength  $\lambda$  (Supplementary Section S1.4 and Supplementary Figure S5). Arrays of microprism devices would offer large overall apertures and large acceptance angles, e.g., for light harvesting applications, as well as large angular alignment tolerances. Translational alignment errors need to be small compared to the wavelengths of interest (Supplementary Section S1.3), implying that larger translational errors relative to the prism size can be tolerated for smaller prisms and longer wavelengths.

In essence, ultimately broadband, complete absorption and rejection of light, as presented here, is a wave interference phenomenon enabled by a layer of substantially sub-wavelength thickness with suitable traveling wave absorption and reflection characteristics. It follows that conceptionally similar black hole wave absorbers and/or white hole wave rejectors may be implemented for all sorts of waves. Indeed, coherent perfect absorption has been reported for electromagnetic waves from microwaves to optical frequencies 16-18 as well as for sound waves. While such works have demonstrated great potential, reliance on complex multi-component interferometers has stood in the way of practical device implementations. By showing how spatial coherence can be exploited to achieve deterministic wavematter interaction – or its deterministic absence – in simple, compact, monolithic, and broadband devices, the concept reported here indicates how the large body of work on thin-film coherent perfect absorption can be translated robustly into practical applications.

## Conclusion

In summary, we have demonstrated how spatial coherence enables broadband deterministic absorption and rejection of light of orthogonal polarizations by simple and compact devices. We describe these as optical black and white holes, as the concept allows for complete absorption and rejection, in principle with unlimited bandwidth, characteristics shared with the black and white holes of general relativity. In practice, a very large bandwidth can be obtained, with limitations arising from the device size (Supplementary Fig. S5) and material dispersion (Supplementary Section S1.2). Our device implementation shows how the large body of work on coherent perfect absorption can be translated into practical devices, such as broadband energy harvesters, polarizers, perfect absorbers (e.g., for stealth technologies), and detectors. The latter could offer high quantum efficiency, directional selectivity, and sensitivity to spatial coherence and polarization. Arising from wave physics, the concept is also applicable to waves outside of electromagnetism, with implications from photonics to acoustics and beyond.

# Data availability

The data shown in the figures are openly available from the University of Southampton ePrints research repository at <a href="https://doi.org/10.5258/SOTON/D2906">https://doi.org/10.5258/SOTON/D2906</a>

# Acknowledgements

This work is supported by the Zepler Institute Stimulus Fund, UK's Engineering and Physical Sciences Research Council (grants EP/M009122/1 and EP/T02643X/1), and Singapore National Research Foundation (NRF2021-QEP2-01-P01). For the purpose of open access, the author has applied a CC BY public copyright license to any Author Accepted Manuscript version arising from this submission.

#### **Author contributions**

N.I.Z. suggested the double prism arrangement of the absorption/rejection device. A.N.V. simulated and fabricated chromium films. E.P. and N. V. designed the experimental setup and conducted the experiments. E.P. derived the analytical description. B.S. conducted finite element method simulations. All authors analyzed the data, wrote and edited the manuscript.

#### **Competing interests**

The authors declare no competing interests.

#### References

- S. Weinfurtner, E. W. Tedford, M. C. J. Penrice, W. G. Unruh, and G. A. Lawrence, "Measurement of stimulated hawking emission in an analogue system," Phys. Rev. Lett. **106**, 021302 (2011).
- M. Visser, "Acoustic black holes: Horizons, ergospheres and hawking radiation," Class. Quantum Grav. **15**, 1767 (1998).
- J. R. Muñoz de Nova, K. Golubkov, V. I. Kolobov, and J. Steinhauer, "Observation of thermal hawking radiation and its temperature in an analogue black hole," Nature **569**, 688-691 (2019).
- D. A. Genov, S. Zhang, and X. Zhang, "Mimicking celestial mechanics in metamaterials," Nat. Phys. **5**, 687-692 (2009).
- E. E. Narimanov and A. V. Kildishev, "Optical black hole: Broadband omnidirectional light absorber," Appl. Phys. Lett. **95**, 041106 (2009).
- T. G. Philbin, C. Kuklewicz, S. Robertson, S. Hill, F. König, and U. Leonhardt, "Fiber-optical analog of the event horizon," Science **319**, 1367-1370 (2008).
- F. Belgiorno, S. L. Cacciatori, M. Clerici, V. Gorini, G. Ortenzi, L. Rizzi, E. Rubino, V. G. Sala, and D. Faccio, "Hawking radiation from ultrashort laser pulse filaments," Phys. Rev. Lett. **105**, 203901 (2010).
- <sup>8</sup> R. A. Tinguely and A. P. Turner, "Optical analogues to the equatorial kerr–newman black hole," Commun. Phys. **3**, 120 (2020).
- Y. Rosenberg, "Optical analogues of black-hole horizons," Phil. Trans. R. Soc. A 378, 20190232 (2020).
- Y. D. Chong, L. Ge, H. Cao, and A. D. Stone, "Coherent perfect absorbers: Time-reversed lasers," Phys. Rev. Lett. **105**, 053901 (2010). doi: 10.1103/PhysRevLett.105.053901.
- <sup>11</sup> W. W. Salisbury, Patent No. US 2599944 (A) (1952).
- H.-T. Chen, "Interference theory of metamaterial perfect absorbers," Opt. Express **20**, 7165-7172 (2012).
- M. A. Kats and F. Capasso, "Optical absorbers based on strong interference in ultra-thin films," Las. Photonics Rev. **10**, 735-749 (2016).
- L. Wu, L. Yang, X. Zhu, B. Cai, and Y. Cheng, "Ultra-broadband and wide-angle plasmonic absorber based on all-dielectric gallium arsenide pyramid nanostructure for full solar radiation spectrum range," Int. J. Therm. Sci. **201**, 109043 (2024).

- Y. Cheng, R. Xing, F. Chen, H. Luo, A. A. Fathnan, and H. Wakatsuchi, "Terahertz pseudowaveform-selective metasurface absorber based on a square-patch structure loaded with linear circuit components," Adv. Photonics Res. **5**, 2300303 (2024).
- J. Zhang, K. F. MacDonald, and N. I. Zheludev, "Controlling light-with-light without nonlinearity," Light Sci. Appl. 1, e18 (2012). doi: 10.1038/lsa.2012.18.
- E. Plum, K. F. MacDonald, X. Fang, D. Faccio, and N. I. Zheludev, "Controlling the optical response of 2d matter in standing waves," ACS Photonics **4**, 3000 (2017).
- D. G. Baranov, A. Krasnok, T. Shegai, A. Alù, and Y. Chong, "Coherent perfect absorbers: Linear control of light with light," Nat. Rev. Mater. **2**, 17064 (2017).
- <sup>19</sup> C. Hägglund, S. P. Apell, and B. Kasemo, "Maximized optical absorption in ultrathin films and its application to plasmon-based two-dimensional photovoltaics," Nano Lett. **10**, 3135-3141 (2010). doi: 10.1021/nl101929j.
- S. Thongrattanasiri, F. H. L. Koppens, and F. J. García de Abajo, "Complete optical absorption in periodically patterned graphene," Phys. Rev. Lett. **108**, 047401 (2012). doi: 10.1103/PhysRevLett.108.047401.
- S. M. Rao, J. J. F. Heitz, T. Roger, N. Westerberg, and D. Faccio, "Coherent control of light interaction with graphene," Opt. Lett. **39**, 5345-5374 (2014). doi: 10.1364/OL.39.005345.
- A. Goodarzi, M. Ghanaatshoar, and M. Mozafari, "All-optical fiber optic coherent amplifier.," Sci. Rep. **8**, 15340 (2018).
- A. N. Vetlugin, R. Guo, C. Soci, and N. I. Zheludev, "Anti-hong—ou—mandel interference by coherent perfect absorption of entangled photons," New J. Phys. **24**, 122001 (2022).
- A. N. Vetlugin, F. Martinelli, S. Dong, and C. Soci, "Photon number resolution without optical mode multiplication," Nanophotonics **12**, (2023).
- <sup>25</sup> C. Yan, M. Pu, J. Luo, Y. Huang, X. Li, X. Maa, and X. Luo, "[invited] coherent perfect absorption of electromagnetic wave in subwavelength structures," Opt. Laser Technol. **101**, 499-506 (2018).
- P. T. Landsberg and G. Tonge, "Thermodynamic energy conversion efficiencies," J. Appl. Phys. **51**, R1-R20 (1980).
- T. Roger, S. Vezzoli, E. Bolduc, J. Valente, J. J. F. Heitz, J. Jeffers, C. Soci, J. Leach, C. Couteau,
  N. I. Zheludev, and D. Faccio, "Coherent perfect absorption in deeply subwavelength films in the single-photon regime," Nat. Commun. 6, 7031 (2015). doi: 10.1038/ncomms8031.
- C. M. X. Altuzarra, S. Vezzoli, J. Valente, W. Gao, C. Soci, D. Faccio, and C. Couteau,
  "Coherent perfect absorption in metamaterials with entangled photons," ACS Photonics 4,
  2124-2128 (2017). doi: 10.1021/acsphotonics.7b00514.
- V. Nalla, S. Vezzoli, J. Valente, H. Sun, and N. I. Zheludev, presented at the CLEO/Europe-EQEC 2015, Munich, Germany, 2015 (unpublished).
- S. Yanikgonul, R. Guo, A. Xomalis, A. N. Vetlugin, G. Adamo, C. Soci, and N. I. Zheludev, "Phase stabilization of a coherent fiber network by single-photon counting," Opt. Lett. **45**, 2740 (2020).
- A. Xomalis, I. Demirtzioglou, E. Plum, Y. Jung, V. Nalla, C. Lacava, K. F. MacDonald, P. Petropoulos, D. J. Richardson, and N. I. Zheludev, "Fibre-optic metadevice for all-optical signal modulation based on coherent absorption," Nat. Commun. **9**, 182 (2018).
- A. N. Vetlugin, R. Guo, C. Soci, and N. I. Zheludev, "Deterministic generation of entanglement in a quantum network by coherent absorption of a single photon," Phys. Rev. A **106**, 012402 (2022).
- M. Papaioannou, E. Plum, and N. I. Zheludev, "All-optical pattern recognition and image processing on a metamaterial beam splitter," ACS Photonics **4**, 217-222 (2017). doi: 10.1021/acsphotonics.6b00921.
- H. Mashaal, A. Goldstein, D. Feuermann, and J. M. Gordon, "First direct measurement of the spatial coherence of sunlight," Opt. Lett. **37**, 3516-3518 (2012).

- M. V. Berry, "The adiabatic phase and pancharatnam's phase for polarized light," J. Mod. Opt. **34**, 1401-1407 (1987).
- M. Lanoy, R.-M. Guillermic, A. Strybulevych, and J. H. Page, "Broadband coherent perfect absorption of acoustic waves with bubble metascreens," Appl. Phys. Lett. **113**, 171907 (2018).
- <sup>37</sup> C. Meng, X. Zhang, S. T. Tang, M. Yang, and Z. Yang, "Acoustic coherent perfect absorbers as sensitive null detectors," Sci. Rep. **7**, 43574 (2017). doi: 10.1038/srep43574.
- P. Wei, C. Croënne, S. T. Chu, and J. Li, "Symmetrical and anti-symmetrical coherent perfect absorption for acoustic waves," Appl. Phys. Lett. **104**, 121902 (2014).
- P. B. Johnson and R. W. Christy, "Optical constants of transition metals: Ti, v, cr, mn, fe, co, ni, and pd," Phys. Rev. B **9**, 5056-5070 (1974).
- J. Pflüger, J. Fink, W. Weber, K. P. Bohnen, and G. Crecelius, "Dielectric properties of ticx, tinx, vcx, and vnx from 1.5 to 40 ev determined by electron-energy-loss spectroscopy," Phys. Rev. B **30**, 1155-1163 (1984).
- A. B. Djurišić and E. H. Li, "Optical properties of graphite," J. Appl. Phys. **85**, 7404-7410 (1999).
- M. R. Querry, "Optical constants," Contractor Report CRDC-CR-85034 (1985).
- A. Banerjee, R. M. Heath, D. Morozov, D. Hemakumara, U. Nasti, I. Thayne, and R. H. Hadfield, "Optical properties of refractory metal based thin films," Opt. Mater. Express 8, 2072 (2018).
- M. Pu, Q. Feng, M. Wang, C. Hu, C. Huang, X. Ma, Z. Zhao, C. Wang, and X. Luo, "Ultrathin broadband nearly perfect absorber with symmetrical coherent illumination," Opt. Express **20**, 2246-2254 (2012). doi: 10.1364/OE.20.002246.
- <sup>45</sup> F. A. Jenkins and H. E. White, *Fundamentals of optics*, 4th ed. (1976).